

Perceived Instability of Virtual Haptic Texture. II. Effect of Collision-Detection Algorithm

*Correspondence to

hongtan@purdue.edu

Abstract

This article reports the second study in a series that investigates perceived instability—unrealistic sensations associated with virtual objects—of virtual haptic texture. Our first study quantified the maximum stiffness values under which virtual haptic textures were perceived to be stable (Choi & Tan, 2004). The present study investigated the effect of the collision-detection algorithm by removing the step changes in force magnitude that could have contributed to perceived instability in the first study. Our results demonstrate a significant increase in the maximum stiffness for stable haptic texture rendering. We also report a new type of perceived instability, aliveness, that is characterized by a pulsating sensation. We discuss the possible cause of aliveness and show that it is not always associated with control instability. Our results underscore the important roles played by environment modeling and human haptic perception, as well as control stability, in ensuring a perceptually stable virtual haptic environment.

I Introduction

Haptic texture rendering is a growing research field that holds much promise for enriching the sensory attributes of objects in a virtual environment and for allowing precise and systematic control of textured surfaces for psychophysical studies. Despite the recent advances in haptic texture rendering (Fritz & Barner, 1996; Massie, 1996; Minsky & Lederman, 1996; Siira & Pai, 1996; Okamura, Dennerlein, & Howe, 1998; Ho, Basdogan, & Srinivasan, 1999; Costa & Cutkosky, 2000; Kim, Kyrikou, Sukhatme, & Desbrun, 2002; Choi & Tan, 2004; Ho, Adelstein, & Kazerooni, 2004), many challenges remain before haptic texture rendering can be widely used in real-world applications.

One problem commonly observed from haptic textures rendered with force-feedback devices is *perceived instability*. Perceived instability refers to all unrealistic sensations (such as buzzing and apparent aliveness of a surface) that cannot be attributed to the physical properties of the textures being rendered. The presence of perceived instability seriously undermines the realism of virtual haptic textures. In order for a haptic texture-rendering system to deliver realistic sensations to human users, it is imperative that we quantify the conditions under which virtual textured objects are free of any perceived artifacts, and that we understand the sources of perceived instability when it occurs.

This article is the second work covering our recent studies of the perceived instability of virtual haptic textures. In our previous work (Choi & Tan, 2004),

we quantified the level of perceived stability/instability of haptic textures using psychophysical experiments. Participants interacted with a textured surface rendered with a PHANToM force-feedback device (SensAble Technologies; Woburn, MA) and judged the maximum stiffness of the surface that could be rendered without perceived instability. Experimental conditions differed in texture model parameter, texture-rendering method, and exploration mode. We found that the parameter space for perceptually stable haptic texture rendering was very small. The stiffest textured surfaces rendered within the stable parameter space felt like soft corduroy, thereby greatly limiting the range of textures that could be rendered without perceptual artifacts. The most prominent type of perceived instability was “buzzing”—a high-frequency noise that occurred in addition to a lower frequency vibration conveying texture information. Further characterization of proximal stimuli (position, force, and acceleration at or near the tip of the PHANToM stylus) revealed that the buzzing sensation was due to a high-frequency signal in the range 192–240 Hz. We demonstrated that the source of this high-frequency noise was most likely the mechanical resonance of the PHANToM.

In this article, we report our recent study on the effect of the collision-detection algorithm on perceived instability of virtual haptic textures. In our previous study (Choi & Tan, 2004), we used a common collision-detection algorithm that was based on the geometrical model of the underlying surface alone (e.g., a plane). Although this method was computationally inexpensive and could be easily extended to nonplanar surface geometry, it nevertheless introduced a step change in rendered force when the stylus of a haptic interface entered and left a textured object surface (see Section 2 for details). This step change in force might have contributed to perceived instability during haptic texture rendering. In the present study, we employed a new algorithm that compared the location of the stylus tip to the texture model superimposed on an underlying flat wall. With the new algorithm, the rendered forces changed continuously near entry points at the cost of increased computational complexity. Other than the

change in collision-detection algorithm, the present study was similar to the previous one in that psychophysical and measurement experiments were performed to quantify the level of perceived stability/instability and to characterize the proximal stimuli responsible for perceived instability, respectively. It was expected that the new collision-detection algorithm would improve the perceived stability of the haptic texture-rendering system, although the extent of the improvement needed to be quantified.

Our work can be placed in the context of achieving perceptually realistic rendering of haptic virtual environments. Typically, haptic interaction occurs at an interaction tool (e.g., the stylus of a haptic interface) that mechanically couples two dynamic systems: the haptic interface with a computer, and the human user with a central nervous system. The model of a virtual environment, the stability of the haptic interface, and the function of our somatosensory system all have a significant effect on the perceived quality of the virtual environment. It follows that at least three requirements need to be satisfied in order for a haptic texture-rendering system to produce realistic textures. First, the virtual-environment dynamics must preserve the essence of the real contact dynamics in order to produce percepts that are consistent with a user’s experience and expectations. Second, the haptic interface has to be stably controlled, thereby generating forces that faithfully follow the force commands determined by the environment dynamics. Finally, the perceived quality of a haptic texture-rendering system should be evaluated by human observers. To the best of our knowledge, only the second requirement (device-control stability) has received much attention from the haptics research community, with a majority of studies focusing on the stability of rendering a flat wall (e.g., see Gillespie & Cutkosky, 1996; Adams & Hannaford, 1999; Lawrence, Pao, Dougherty, Salada, & Pavlou, 2000; Miller, Colgate, & Freeman, 2000; Çavuşoğlu, Sherman, & Tendick, 2002; Hannaford & Ryu, 2002). Our previous work showed that buzzing, a form of perceived instability, was indeed due to control instability (high-frequency unstable modes of the PHANToM; Choi & Tan, 2004). Our present work

will demonstrate that another type of perceived instability, “aliveness,” is due to inaccurate environment modeling and can occur even when the haptic interface is passive (hence stable in the control sense). Therefore, our work stresses the importance of studying the role that environment modeling plays in rendering haptic virtual environments. By using human observers in all our studies, we also ensure that our results reflect the role that perception plays in a user’s interaction with virtual environments.

The remainder of this article is organized as follows: Section 2 provides the background for collision-detection algorithms in haptic texture rendering. We then present the design and results of psychophysical experiments in Section 3. In Section 4, we present the proximal stimuli (position, force, and acceleration) measured at the PHANTOM stylus and discuss the sources of two types of perceived instabilities. We conclude the article in Section 5 with a discussion on the implications of our work for rendering virtual environments.

2 Collision Detection in Haptic Texture Rendering

In general, the detection of a collision between an interaction tool of a haptic interface and virtual objects is a computationally complex and expensive task that has to be executed within a fraction of the haptic update interval. A collision-detection problem is usually reduced to finding a point on an object surface that is closest to the position of the interaction tool. Many collision-detection algorithms for efficient haptic rendering have been studied for general geometrical-object models such as polygonal and NURBS models (see Lin & Manocha, 2004, for a review).

Collision detection becomes much more complex once textures (microgeometry of objects) are mapped onto the object surfaces. For simplicity of further discussion, we assume that the shape (macrogeometry) of the virtual objects is modeled using polygons. Difficulty in collision detection for textured objects arises from two sources. One is the mathematical complexity associ-

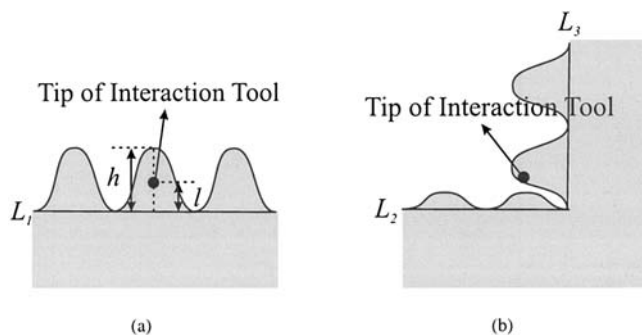


Figure 1. Examples of (a) successful and (b) unsuccessful collision detection involving textured virtual objects.

ated with the representation of textured object surfaces. Iterative numerical algorithms are often required to determine a point on a textured surface with a minimum distance from the interaction tool. The computation time required for a well-converged solution can be too long to be useful for haptic rendering. The other difficulty is the lack of a global representation of the boundaries of the textured virtual objects. In a typical implementation, the polygons and the texture model are stored at separate locations in computer memory. The texture model is locally mapped onto a point on the polygon for calculating the perturbed height and/or normal at that point. It is often infeasible to search for a global minimum using only the local information.

Few studies have explicitly considered the problem of collision detection in haptic texture rendering, except for Ho et al. (1999). Their algorithm finds a minimum-distance point using a two-step approach. In the first step, which considers only the underlying polygons, a polygon with a minimum distance from the tip of the interaction tool is determined (for example, polygon L_1 in Figure 1a). In the second step, which also takes into account the texture model, the distance between the polygon and the tool tip (l) is compared to the height of the texture model projected on the normal of the polygon (h) to determine whether a collision has occurred. This algorithm works well when the tool tip is not too close to the edges of polygons. However, it can fail if the interaction tool is in contact with a bump on

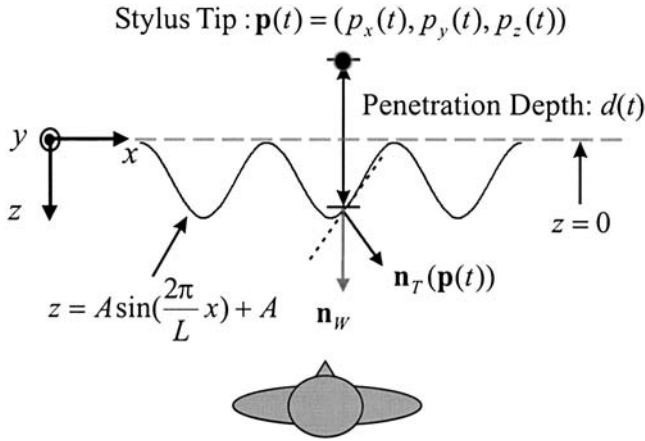


Figure 2. Illustration of parameters used in texture rendering. All variables are defined in the world coordinate frame of the force-feedback display.

another polygon, instead of a bump on top of the polygon found by the minimum-distance criterion in the first step. For example, as shown in Figure 1(b), the algorithm would fail to detect a collision between the tool tip and polygon L_3 , because L_2 is closer to the tool tip than L_3 . To the best of our knowledge, no general solution has been proposed for collision detection in haptic texture rendering.

The textured object used in our study is shown in Figure 2. The user explored a vertical textured plane represented by $z = A \sin\left(\frac{2\pi}{L}x\right) + A$ with a stylus. This textured plane was formed by superimposing the 1D sinusoidal texture model on the underlying plane located at $z = 0$. The position of the tip of the PHANToM stylus was denoted by $\mathbf{p}(t) = (p_x(t), p_y(t), p_z(t))$ in the figure. In our first study (Choi & Tan, 2004), collision detection was based on the z -coordinate of the stylus position and the underlying flat wall. Penetration depth was calculated as

$$d_1(t) = \begin{cases} 0 & \text{if } p_z(t) > 0 \\ b(p_x(t)) - p_z(t) & \text{if } p_z(t) \leq 0, \end{cases} \quad (1)$$

where $b(p_x(t)) = A \sin\left(\frac{2\pi}{L}p_x(t)\right) + A$ was the height of the texture model at $p_x(t)$, as shown in Figure 2. In the

present study, collision detection was performed on the boundary defined by the sinusoidal textured surface. Penetration depth was calculated as

$$d_2(t) = \begin{cases} 0 & \text{if } p_z(t) > b(p_x(t)) \\ b(p_x(t)) - p_z(t) & \text{if } p_z(t) \leq b(p_x(t)). \end{cases} \quad (2)$$

Since $d_1(t)$ uses an underlying flat surface for assessing collision detection with a textured surface, this method can be easily extended to the rendering of textured objects whose shape is represented by polygons. The problem is that $d_1(t)$ produces a step change in rendered forces when the PHANToM stylus enters and leaves the textured plane. The new algorithm $d_2(t)$ avoids this problem by considering the explicit representation of the texture model. When the PHANToM stylus remains below the plane defined by $z = 0$, as is often the case when the user strokes the textured surface, the penetration depths calculated by the two methods are the same.

3 Psychophysical Experiment: Quantification of Perceived Instability

This section presents the design and results of psychophysical experiments conducted to quantify the level of perceived stability/instability during haptic texture rendering. We also summarize the types of perceived instability experienced by human observers. Due to the similarity in experiment design between our previous (Choi & Tan, 2004) and present studies, we focus our description of the methods on the differences between the two studies. Interested readers are referred to our previous study for further details.

3.1 Method

3.1.1 Apparatus. A PHANToM force-reflecting haptic interface (model 1.0A with a stylus and an encoder gimbal) was used in all experiments to render virtual textured surfaces. This device has a nominal maximum stiffness of 3.5 N/mm, and a nominal position resolution of 0.03 mm.

3.1.2 Participants. Four participants (2 males, S1 and S4, and 2 females, S2 and S3) participated in the experiments. S1 and S2 had participated in our previous experiments (Choi & Tan, 2004). S1, S3, and S4 were experienced users of the PHANToM device, although S4 was not familiar with virtual haptic textures before his participation in this study. S2 had not used any haptic interface prior to her participation in Choi and Tan (2004). S1 and S3 were members of our research laboratory, S4 was a Purdue graduate student, and S2 was not affiliated with Purdue. Both S2 and S4 were paid for their participation in the present study. The average age of the participants was 30 years old. All participants are right-handed and reported no known sensory or motor abnormalities with their upper extremities.

3.1.3 Stimuli. As shown earlier in Figure 2, the virtual textured surfaces were modeled as 1D sinusoidal gratings with amplitude A and spatial wavelength L , superimposed on a flat surface. Sinusoidal gratings have been widely used as basic building blocks for textured surfaces in studies of haptic texture perception (e.g., Lederman, Klatzky, Hamilton, & Ramsay, 1999; Weisenberger, Krier, & Rinker, 2000) and as a basis function set for modeling real haptic textures (e.g., Wall & Harwin, 1999).

Two texture-rendering methods based on Massie (1996) [denoted by $\mathbf{F}_{mag}(t)$] and Ho et al. (1999) [denoted by $\mathbf{F}_{rec}(t)$] were employed. The two methods produced the same force magnitude of $K \cdot d_2(t)$, where K was the surface stiffness and $d_2(t)$ was the penetration depth as defined in Equation 2. The $\mathbf{F}_{mag}(t)$ method rendered a force with a constant direction that was normal to the underlying flat wall (\mathbf{n}_W in Figure 2). The $\mathbf{F}_{rec}(t)$ method rendered a force in a direction that stayed normal to the sinusoidal textured surface [$\mathbf{n}_T(\mathbf{p}(t))$ in Figure 2]. The main difference between the stimuli used in the present study and those used in Choi and Tan (2004) was the way in which penetration depth was calculated. While the previous study used $d_1(t)$ in Equation 1 for penetration-depth computation, the present study employed $d_2(t)$ in Equation 2.

The stimuli used in the present study were uniquely defined by the amplitude (A) and wavelength (L) of the

sinusoidal texture model, the surface stiffness (K), and the texture-rendering method.

3.1.4 Experimental Conditions. Two exploration modes, free exploration and stroking, were tested in order to examine the effect of participants' interaction patterns on perceived instability. In the free-exploration mode, the participants were allowed to use the interaction pattern that they found most effective at detecting instability of virtual textures. In the stroking mode, the participants were instructed to move the stylus laterally across the textured surface.

Four experiments, defined by the combinations of the two texture-rendering methods and the two exploration modes, were conducted (see Table 1). There were five A and L combinations per experiment. The dependent variable was the maximum stiffness below which the rendered textured surface was perceived to be stable.

3.1.5 Procedure. The experimental procedure was essentially the same as that employed in Choi and Tan (2004). The method of limits was used to estimate the stiffness thresholds. Based on preliminary results, the maximum stiffness (K_{max}) was set to 1.0 N/mm and 1.6 N/mm for free exploration (Experiments I and III) and stroking (Experiments II and IV), respectively. The stiffness increment ΔK was fixed at 0.05 N/mm for all conditions. The order of the four experiments as well as that of the five experimental conditions within each experiment was randomized for each participant. The participant's task was to report whether the virtual textured surface exhibited any perceived instability. Figure 3 shows the experimental setup.

3.2 Results

Stiffness thresholds (denoted by K_T) for the 4 participants are shown in Figure 4. Each panel shows, for 1 participant, the average stiffness thresholds and the corresponding standard errors for each experimental condition. The stiffness thresholds averaged across the participants for Experiments I, II, III, and IV ranged 0.2081–0.5208 N/mm, 0.2310–0.7241

Table 1. *Experimental Conditions for the Psychophysical Experiments*

Experiment	Texture-rendering method	Exploration mode	Texture model parameters A (mm), L (mm)
I	$F_{mag}(t)$	Free exploration	(0.5, 2.0), (1.0, 1.0), (1.0, 2.0), (1.0, 4.0), (2.0, 2.0)
II	$F_{mag}(t)$	Stroking	(0.5, 2.0), (1.0, 1.0), (1.0, 2.0), (1.0, 4.0), (2.0, 2.0)
III	$F_{vec}(t)$	Free exploration	(0.5, 2.0), (1.0, 1.0), (1.0, 2.0), (1.0, 4.0), (2.0, 2.0)
IV	$F_{vec}(t)$	Stroking	(0.5, 2.0), (1.0, 1.0), (1.0, 2.0), (1.0, 4.0), (2.0, 2.0)

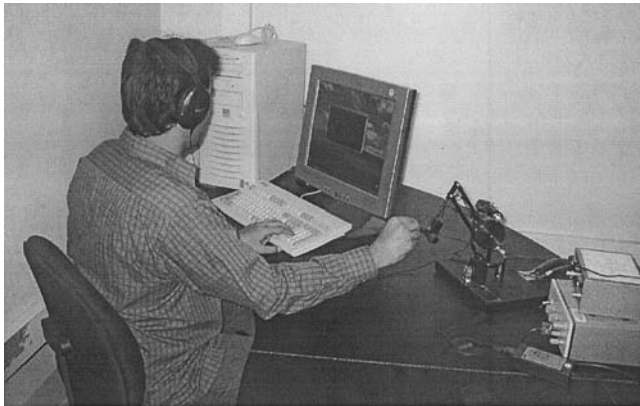
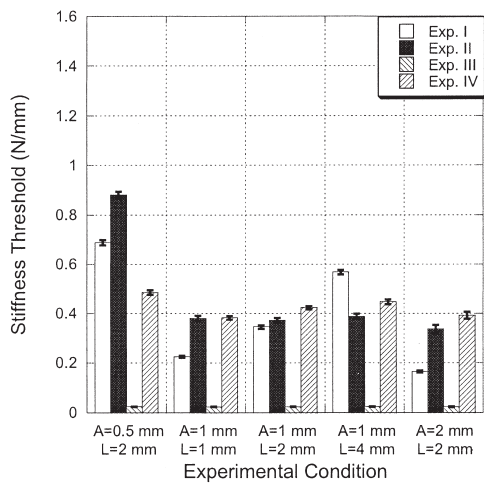


Figure 3. *Experimental setup. Participants explored virtual haptic textures with their right hands using lateral stroking motions. They looked at a computer monitor that contained text information on the current trial number, and looked away from the PHANTOM. Audio noise was delivered through earphones to mask any sound emanating from the PHANTOM.*

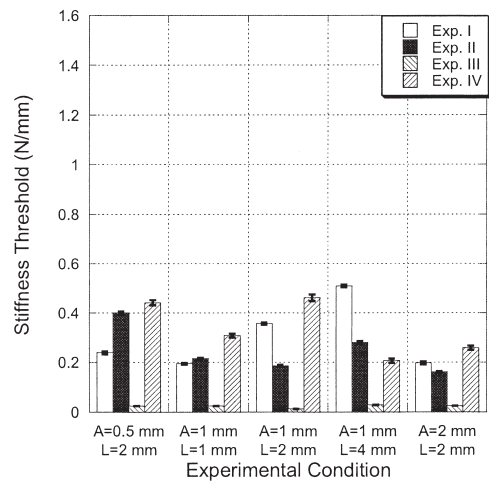
N/mm, 0.0216–0.0256 N/mm, and 0.3571–0.7754 N/mm, respectively.

Despite significant interparticipant differences, the effect of the four factors (texture-rendering method, exploration mode, and amplitude and wavelength of the sinusoidal texture model; see Table 1) can be observed from the data shown in Figure 4. The most obvious trend is that the thresholds from Experiment III [$F_{vec}(t)$, free exploration] were essentially 0 (less than

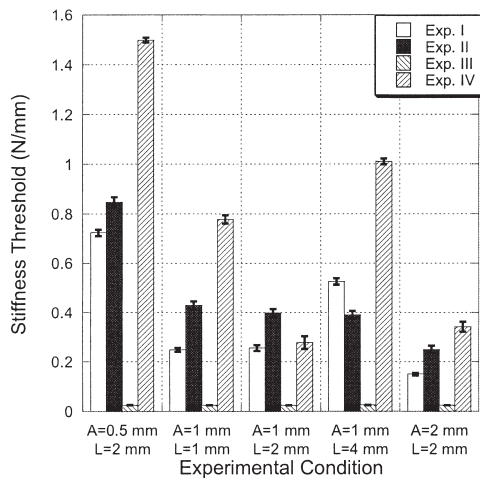
$\Delta K = 0.05$ N/mm), indicating that the participants judged all virtual textures rendered in Experiment III to contain unrealistic sensations. A comparison of thresholds obtained in Experiment I [$F_{mag}(t)$, free exploration] and Experiment III shows that when free exploration was permitted, virtual textured surfaces rendered with $F_{mag}(t)$ resulted in much larger stiffness thresholds than those with $F_{vec}(t)$ for every participant and every combination of A and L tested. However, when stroking was the method of exploration, there was no clear trend of whether $F_{mag}(t)$ (Experiment II) resulted in larger stiffness thresholds than $F_{vec}(t)$ (Experiment IV) or vice versa. On the average, the thresholds obtained in Experiment IV were slightly larger than those in Experiment II by 0.1256 N/mm. This difference was statistically significant, $t(3998) = 34.58$ and $p < .0001$. For the rendering method of $F_{mag}(t)$, it is not clear which of the two exploration modes (Experiments I and II) resulted in more stable virtual textures. On the average, stiffness thresholds associated with stroking (Experiment II) were larger than those associated with free exploration (Experiment I) by 0.0346 N/mm, ($t(3998) = 14.75$ and $p < .0001$). The trend in the data was more apparent for the $F_{vec}(t)$ method. Stroking clearly resulted in much larger stiffness thresholds (Experiment IV) than free exploration (Experiment III), mainly due to the fact that the thresholds obtained from Experiment III were very small. As far as the A and L param-



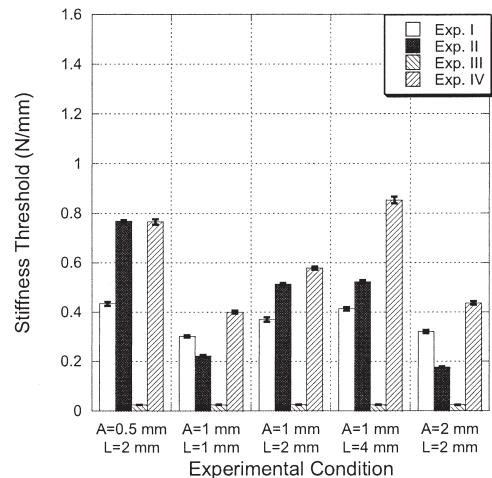
(a) S1



(b) S2



(c) S3



(d) S4

Figure 4. Results of the psychophysical experiments from the present study. Data for the four participants are shown in four separate panels. Each panel shows the average stiffness thresholds and the corresponding standard errors for each of the 20 (4 experiments \times 5 conditions per experiment) experimental conditions tested.

ters are concerned, decreasing A or increasing L generally increased the stiffness thresholds in most cases, except for Experiment III, where the stiffness thresholds were too small to exhibit any patterns. The effect of A can be easily observed in each of the panels by compar-

ing the corresponding stiffness thresholds for the same L values (the first, third, and fifth conditions). The effect of L can be extracted by comparing the thresholds for the same A values (the second, third, and fourth conditions).

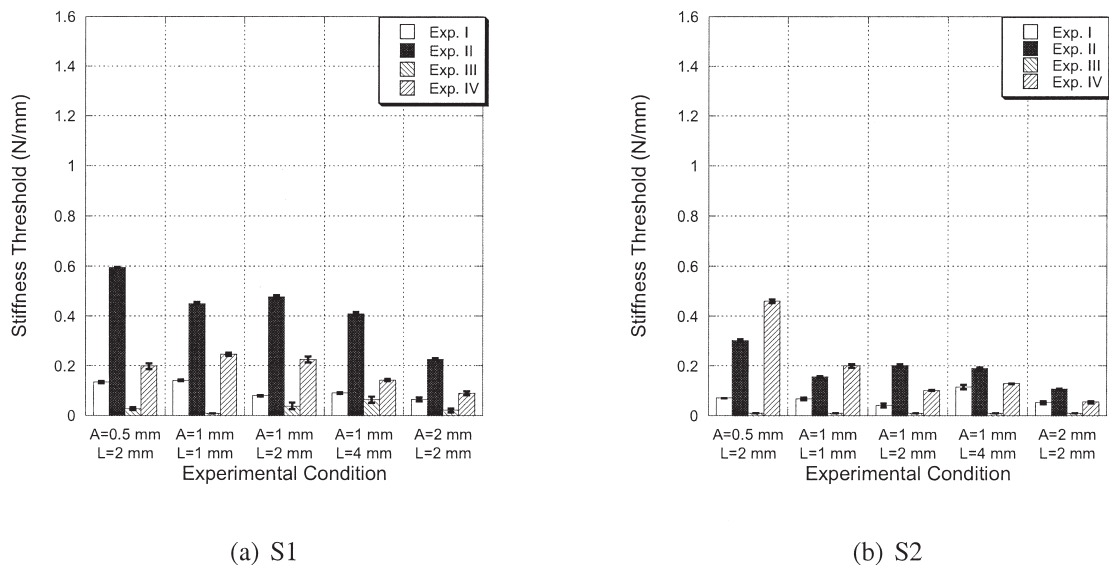


Figure 5. Stiffness thresholds from Choi and Tan (2004) for S1 and S2, who participated in both our previous and present studies. Each panel shows the average stiffness thresholds and the corresponding standard errors for each of the 20 (4 experiments \times 5 conditions per experiment) experimental conditions tested.

3.3 Discussion

In the psychophysical experiments, we measured the maximum stiffness values under which a virtual textured surface rendered with a force-feedback device was perceptually “clean” and stable. The collision-detection algorithm employed in this study was based on the relative positions of the stylus tip and the height of the sinusoidal surface texture (Equation 2). The experimental conditions used in these experiments were a subset of those used in our previous study (Choi & Tan, 2004) in which we employed a collision-detection algorithm based on the relative positions of the stylus tip and the flat wall underlying the textured surface (Equation 1). We can examine the effect of collision-detection algorithms on the perceived quality of virtual haptic textures by comparing the results from our previous and present experiments.

Figure 5 presents the stiffness thresholds measured in our previous experiment where $d_1(t)$ was used for collision detection. Only the data from S1 and S2, who participated in both studies, are shown in the figure. The effect of collision-detection algorithm on stiffness

thresholds can be observed by comparing Figure 4(a) with 5(a), and Figure 4(b) with 5(b), respectively. From the data obtained in Experiments I and IV, it is clear that the use of $d_2(t)$ significantly increased the stiffness thresholds for both participants (average difference = 0.2687 N/mm and 0.1960 N/mm, respectively; $t(3998) = 62.68$ and 40.07 , respectively; $p < .0001$ for both experiments). The stiffness thresholds obtained in Experiment III remained quite small for both participants regardless of the collision-detection algorithm (average difference = 0.0026 N/mm, $t(3998) = 1.17$, $p = .2403$). The trend in results from Experiment II was not very clear by visual inspection. On the average, the stiffness thresholds increased slightly by 0.0487 N/mm when $d_2(t)$ was used. The difference was statistically significant, $t(3998) = 7.447$, $p < .0001$. Numerically, however, only the threshold increases in Experiments I and IV were substantial.

The observed effects of collision-detection algorithms on perceived instability were consistent with our initial expectations for data obtained in Experiments I and III, but not for those obtained in Experiments II and IV. In

Experiment I [$\mathbf{F}_{mag}(t)$, free exploration] and Experiment III [$\mathbf{F}_{vec}(t)$, free exploration], the participants were allowed to explore the virtual haptic textures freely, including moving the PHANToM stylus in and out of the virtual surfaces. Recall that the main difference between the collision-detection algorithms used in the current and previous experiments was that the new algorithm rendered forces that were continuous at the boundary of the virtual textured surfaces. We therefore expected higher stiffness thresholds for Experiments I and III in the present study. The results from Experiment I confirmed our expectation. The stiffness thresholds obtained in Experiment III, however, were uniformly low (i.e., below the step size of 0.05 N/mm used in the method of limits). The participants reported that they felt high-frequency buzzing noises whenever the stylus was positioned inside the textured surfaces. The same was also frequently observed in our previous study (Choi & Tan, 2004). This fact indicates that the rapid changes in force directions due to $\mathbf{F}_{vec}(t)$ significantly decreased the perceived stability of virtual textures to the extent that any improvement in stability due to the new collision-detection algorithm could not be observed.¹ In Experiment II [$\mathbf{F}_{mag}(t)$, stroking] and Experiment IV [$\mathbf{F}_{vec}(t)$, stroking], the participants were instructed to move the PHANToM stylus laterally across the virtual haptic textures. Assuming that the participants kept the stylus inside the textured surface during stroking, we did not expect to observe any significant changes in stiffness thresholds with the new collision-detection algorithm. The results from Experiments II and IV, however, demonstrated statistically significant increases in the mean stiffness thresholds. To seek an explanation for this unexpected result, we examined the position data measured from these two experiments, and report our findings in Section 4.4.

¹ The authors of the $\mathbf{F}_{vec}(t)$ rendering method (Ho et al., 1999) were aware of the instability problem, and developed a heuristic algorithm that interpolated the direction of a force vector between the normal to the texture model (for small penetration depth) and the normal to the underlying surface (for large penetration depth). We were interested in investigating the generic performance of $\mathbf{F}_{vec}(t)$ and therefore did not incorporate the interpolation scheme in our experiments on perceived instability.

The types of sensations associated with perceived instability were discussed through debriefing. The sensations seemed to depend more on how the forces were rendered than on exploration mode. In Experiments I and II [both using $\mathbf{F}_{mag}(t)$], when the stiffness values were well above the measured thresholds, the participants felt high-frequency buzzing noises and used that sensation to judge the virtual texture to be unstable. The same phenomenon was also frequently observed in our previous experiments (Choi & Tan, 2004). When the values of surface stiffness were lowered to be slightly above the measured thresholds, however, the participants often reported that the textured surfaces appeared to be “alive.” Very often, the participant felt force perturbations that could not be attributed to any movements that they had initiated. This type of perceived instability was not observed in our previous study. The sensations associated with perceived instability in Experiments III and IV [both using $\mathbf{F}_{vec}(t)$] were very similar to those reported in our previous study. The two major types of sensations were buzzing and “ridge instability.” The latter describes the phenomenon where the net force exerted by the PHANToM on the stylus tip pointed toward a valley of the sinusoidal gratings when a participant attempted to rest the stylus on a ridge. More details can be found in Choi and Tan (p. 405).

The results of the psychophysical experiments showed that the choice of a collision-detection algorithm clearly influenced the perceived stability/instability of virtual haptic textures. A new type of perceived instability, aliveness, was also observed. In order to gain further insight into how the two types of perceived instability (buzzing and aliveness) depended on the collision-detection algorithm and other factors, we measured the proximal stimuli at the PHANToM stylus under a variety of conditions and report the results in the next section.

4 Measurements: Characterization of Proximal Stimuli

In this section, we report the results of measurement experiments that identified the proximal stimuli

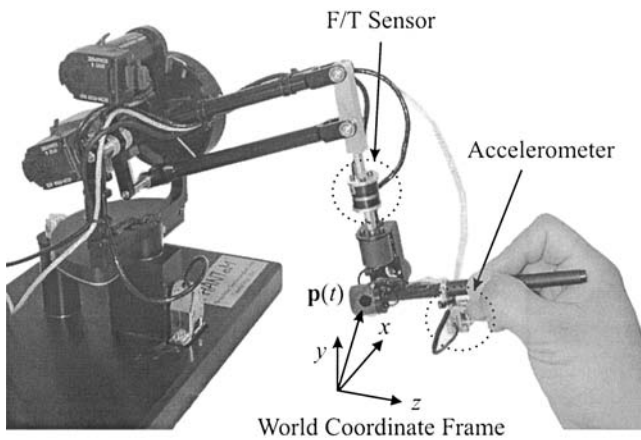


Figure 6. The instrumented PHANToM. A triaxial force/torque (F/T) sensor (ATI Industrial Automation, Apex, NC, model Nano 17 with temperature compensation) was inserted into the last link of the device. A triaxial accelerometer (Kistler, Blairsville, PA, model 8794A500) was attached to the stylus. Further details can be found in Choi and Tan (2004).

responsible for perceived instability. After presenting the methods used in the measurement experiments, we focus our discussion on the following issues:

- Was buzzing caused by high-frequency signals, as was the case in our previous study using the $d_1(t)$ collision-detection algorithm?
- What proximal stimuli were responsible for the perception of aliveness?
- Why did stiffness thresholds increase significantly, albeit unexpectedly, in Experiments II and IV?
- Was aliveness perception caused by device instability, as was the case with buzzing (Choi & Tan, 2004)?

4.1 Method

The PHANToM force-reflecting device instrumented with two additional sensors (a force/torque sensor and an accelerometer) was used for haptic texture rendering and data collection (see Figure 6). This instrumented PHANToM was capable of sensing 3D position, force, and acceleration of the stylus.

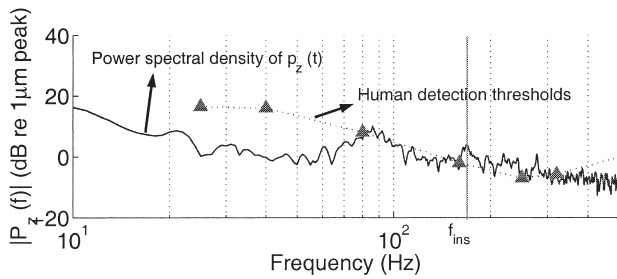
Two participants (S1 and S3) were tested in the mea-

surement experiment. Both participants were experienced users of the PHANToM device. They were preferred over naive participants because they were required to place or move the stylus in a particular manner in order to maintain well-controlled conditions during data collection.

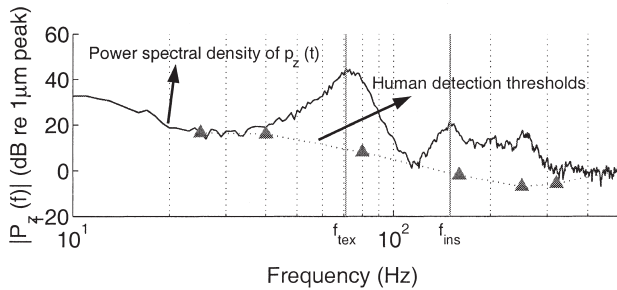
Experimental conditions used in the measurement experiment differed in texture-rendering parameter (A and L), texture-rendering method [$F_{mag}(t)$ and $F_{vec}(t)$], exploration mode (free exploration and stroking), and perceptual category (stable and unstable). The values of surface stiffness (K) were selected to result in either perceptually stable or unstable rendering based on the results of the psychophysical experiments.

For the experiments with free-exploration mode, the participants were instructed to hold the stylus stationary near or deep inside the textured surface. They had to find a point in space where the textured surface was clearly perceived to be unstable and maintain that position. Once the participant was satisfied with the selected stylus position, the experimenter initiated data collection. For the experiments with stroking mode, the participants were instructed to move the stylus laterally across the virtual gratings. They were required to maintain a constant stroking speed to the best of their ability. After the participant had initiated stroking, the experimenter started data collection. In all experimental conditions, the participants were asked to hold the stylus like a pen (see Figure 6). During each trial, 3D position, force, and acceleration data were collected for 10 seconds at a sampling rate of 1 kHz.

Each segment of 10-s-long measured data was analyzed in both time and frequency domains. In the frequency-domain analysis of stroking condition, the location of the spectral peak corresponding to texture information was estimated by $\hat{f}_{tex} = |\bar{v}_x|/L$, where $|\bar{v}_x|$ was the average stroking velocity. The actual frequency (f_{tex}) was then determined from the spectral peak closest to \hat{f}_{tex} in the recorded data. The perceived magnitude of any spectral component was converted from its physical unit to “sensation level” by taking the difference between the log of its intensity and the log of the human detection threshold at the same frequency. See Choi and Tan (2004) for further details.



(a) Spectral density of position data measured with $\mathbf{F}_{mag}(t)$ and free exploration ($A = 1.0$ mm, $L = 2.0$ mm, and $K = 1.0$ N/mm).



(b) Spectral density of position data measured with $\mathbf{F}_{mag}(t)$ and stroking ($A = 1.0$ mm, $L = 2.0$ mm, and $K = 1.2$ N/mm).

Figure 7. Illustration of high-frequency noise associated with the “buzzing” type of perceived instability.

4.2 Was Buzzing Caused by High-Frequency Signals?

Buzzing often occurred when a high stiffness value was used in haptic texture rendering. In our measured data, we were able to observe a high-frequency spectral peak whenever buzzing was perceived. Figure 7 provides an example of the high-frequency noise associated with the perception of buzzing for (a) free exploration and (b) stroking. In both panels, the spectral densities for position signal $p_z(t)$ (perpendicular to the wall underlying the textured surface) are shown as solid lines, and the human detection thresholds are shown as dashed lines with triangles (reproduced from Verrillo,

1963; see Choi & Tan, 2004 for why these thresholds were chosen for comparison). The data shown in Figure 7(a) were taken with the stylus tip positioned near the textured surface [$\mathbf{F}_{mag}(t)$, free exploration, buzzing]. We can observe several spectral peaks at a frequency of 169 Hz (marked f_{ins} for instability frequency) or higher. The intensity of the spectral peaks was as much as 7 dB above human detection thresholds, indicating that they could be perceived by our participants. We therefore conclude that these high-frequency spectral components contributed to the perception of buzzing.

Figure 7(b) shows data recorded while the participant stroked the textured plane [$\mathbf{F}_{mag}(t)$, stroking, buzzing]. We can observe one spectral peak at 71 Hz (marked f_{tex} for texture frequency) and several spectral peaks at 150 Hz (marked f_{ins}) and higher. The location of f_{tex} was consistent with that estimated from the spatial wavelength L of the texture model and the measured average stroking velocity $|\bar{v}_x|$. Therefore, this spectral component provided the temporal cues for the perception of the textured surface during stroking. The high-frequency spectral peaks were as much as 25 dB above human detection thresholds and therefore contributed to a strong sensation of buzzing.

Results obtained with textured surfaces rendered with $\mathbf{F}_{vec}(t)$ exhibited similar high-frequency spectral peaks whenever buzzing was perceived. Taken together, the measurement data obtained in the current study were consistent with those obtained in our previous study (Choi & Tan, 2004) in that high-frequency spectral peaks with intensities well above human detection thresholds were responsible for the perception of buzzing that made virtual haptic textures feel unstable. Therefore, the choice of a collision-detection algorithm did not change the underlying cause for the perception of buzzing.

4.3 What Signals Were Responsible for Aliveness?

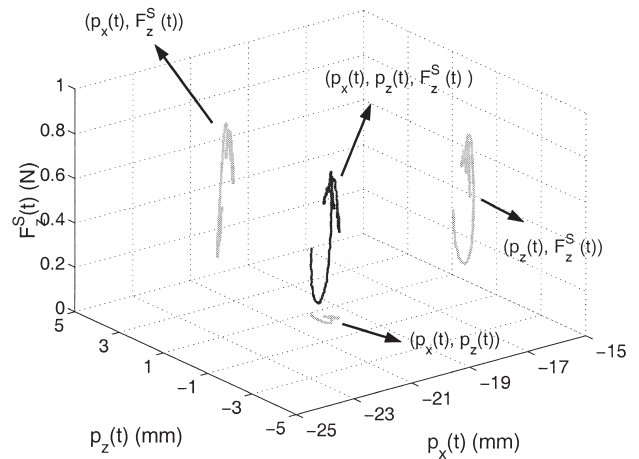
When the stiffness of the textured surface rendered using $\mathbf{F}_{mag}(t)$ was slightly above the threshold for stable texture rendering, the participants reported that the apparent aliveness of the surface became the domi-

nant cue for perceived instability. Consistent with the participants' observation, no prominent high-frequency spectral peaks were observed in the power spectral densities of recorded data (measured with stiffness values one standard deviation above the thresholds). Instead, we found many instances where a relatively large force variation occurred while the PHANToM stylus barely moved along the direction of the force variation. Figure 8 illustrates this finding with position and force data measured during (a) free exploration and (b) stroking. In both panels, force variation along the cylindrical axis of the stylus, $F_z^S(t)$, is plotted against the displacement of the stylus in two directions, $p_x(t)$ (along the direction of stroking) and $p_z(t)$ (along the direction of surface-height variation), for a period of 400 ms. Also shown in both panels of Figure 8 are the three projections of measured force. We did not plot $F_z^S(t)$ against $p_y(t)$ since our texture model did not vary along the y -axis.

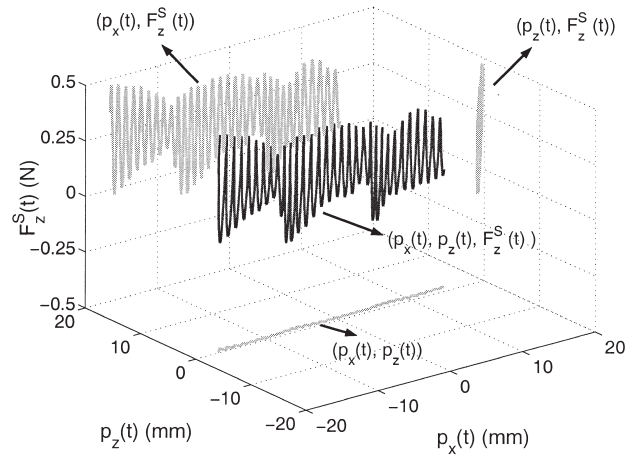
The data shown in Figure 8(a) were taken with the stylus tip held stationary near the textured surface [$\mathbf{F}_{mag}(t)$, free exploration]. The projection on the $p_x(t) - p_z(t)$ plane shows that the stylus tip moved by less than 0.56 mm and 0.94 mm in the x and z directions, respectively. These movement magnitudes are barely perceivable when the hand is held in free space.² The corresponding change in force magnitude, however, was large enough to be clearly perceived, $\max F_z^S(t) - \min F_z^S(t) = 0.59$ N. Since the participant was under the impression that the PHANToM stylus was held still in space, the perceived force variation was attributed to an alive virtual textured surface rather than to the slight tremor of the participant's hand.

The same phenomenon can be observed in Figure 8(b) with data collected during stroking [$\mathbf{F}_{mag}(t)$, stroking]. In this figure, the large change in $p_x(t)$ was the result of the participant's stroking movement. While the force data [$F_z^S(t)$] felt by the participant exhibited magnitude variations on the order of 0.5 N, the change in position along the direction of surface-height variation [$p_z(t)$] was hardly perceptible (less than 1 mm). As a

² We were not able to find detection thresholds for hand movement in free space in the literature to compare these numbers against.



(a) Force and position data measured with $\mathbf{F}_{mag}(t)$ and free exploration ($A = 1.0$ mm, $L = 1.0$ mm, and $K = 0.4$ N/mm).



(b) Force and position data measured with $\mathbf{F}_{mag}(t)$ and stroking ($A = 1.0$ mm, $L = 1.0$ mm, $K = 0.5$ N/mm).

Figure 8. Characteristics of aliveness.

result, the participant felt a noticeable force change through the stylus although the stylus was perceived to be barely moving in and out of the textured surface. It follows that this force variation was interpreted as coming from an alive textured surface. The participants also reported that they felt the surface “pulsating” during stroking.

4.4 Why Did Stiffness Thresholds Increase in Experiments II and IV?

Recall that the main difference between the two collision-detection algorithms $d_1(t)$ and $d_2(t)$ was that $d_1(t)$ introduced step changes at the entry points along the textured surface but $d_2(t)$ did not. Also recall that the two psychophysical Experiments II and IV employed stroking mode. To the extent that the PHANToM stylus remained underneath the textured surface during stroking, we did not expect to see a significant increase in stiffness thresholds in the present study using $d_2(t)$. However, it was found that stiffness thresholds increased significantly in both Experiment II [$\mathbf{F}_{mag}(t)$, stroking] and Experiment IV [$\mathbf{F}_{vec}(t)$, stroking].

In order to explain the increase in threshold, we examined the stylus positions recorded during these two experiments. Figure 9 shows typical data traces for $p_x(t)$ (position along the stroking direction), $p_z(t)$ (position along the surface-height variation), and the calculated penetration depth $d_1(t)$ (panels a and b) or $d_2(t)$ (panels c and d). Also shown with $p_z(t)$ (solid line in the middle of each panel) are the height of the sinusoidal textured surface computed at $p_x(t)$ (dash-dotted line in the middle of each panel), and the underlying wall (straight dashed line). The duration of each data trace is 500 ms. It can be seen from the $p_z(t)$ traces of Figures 9(a) and 9(b) that the stylus remained near or below the textured surface at all times with the $d_1(t)$ collision-detection algorithm. From the $p_z(t)$ traces of Figure 9(c) and 9(d), it is obvious that the stylus did not remain inside the textured surface at all times. Instead, the stylus was somewhere between the peaks and valleys of the sinusoidal height variations. Therefore, our assumption that the stylus remained inside the textured surfaces during stroking was not valid. Furthermore, we observe from the $d_2(t)$ traces of Figures 9(c) and 9(d) that there were no abrupt step changes in the calculated penetration depths, and therefore no abrupt changes in the calculated force commands either. These measurements explain why the stiffness thresholds obtained in Experiments II and IV increased significantly in the current study.

4.5 Was Aliveness Caused by Device Instability?

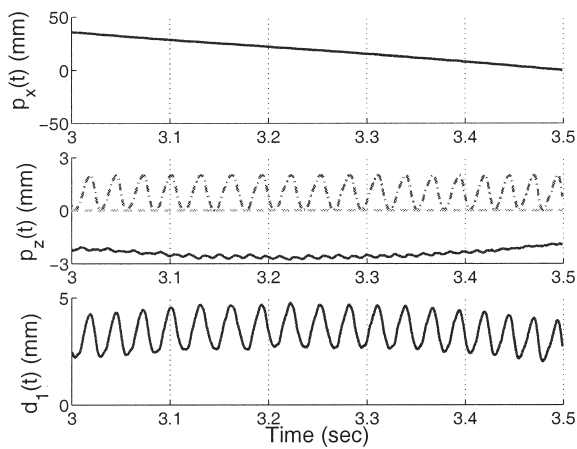
Of the three main factors affecting the perceived stability of virtual haptic textures (environment modeling, device-control stability, and human perception), which factor(s) would explain the phenomenon of aliveness? To investigate this question, we examined whether it was possible for a human user to perceive aliveness while the texture-rendering system including the force-feedback device was stable in the control sense. For this purpose, we applied a passivity-based stability theory on the data measured from a user interacting with virtual textured surfaces. We examined whether aliveness could be perceived from a passive (thereby stable) texture-rendering system. The passivity of our texture-rendering system was evaluated with a passivity observer (PO), an on-line observer for monitoring the energy flow of a dynamic system (Hannaford & Ryu, 2002).

For the texture-rendering system shown in Figure 10, the PO with no initial energy storage was defined as

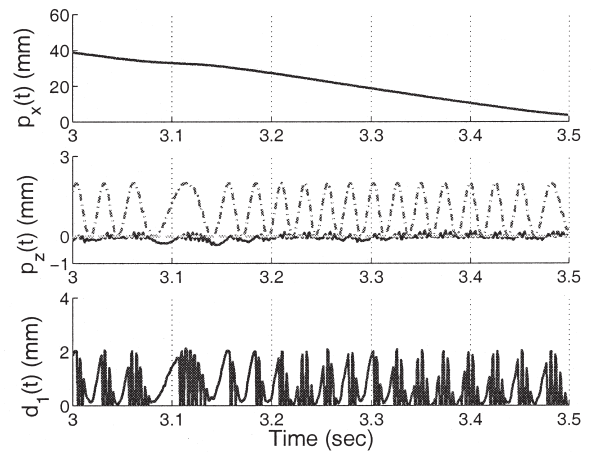
$$PO(k) = \sum_{i=1}^k \mathbf{F}_z^W(i\Delta t) \nu_z(i\Delta t) \Delta t, \quad (3)$$

where Δt was the sampling period, k was the time index for samples, $\mathbf{F}_z^W(t)$ was the measured force at the PHANToM stylus along the z -axis of the PHANToM world coordinate frame, and $\nu_z(t)$ was the velocity of the stylus along the z -axis. The forces and velocities in the other directions were not considered since the $\mathbf{F}_{mag}(t)$ rendering method produced forces only in the z -direction. Due to the poor resolution of velocity estimates derived directly from the PHANToM position encoders (Çavuşoğlu, Feygin, & Tendick, 2002), $\nu_z(t)$ was estimated using an end-fit first-order adaptive windowing technique (Janabi-Sharifi, Hayward, & Chen, 2000). The texture-rendering system was considered to be passive if the PO remained positive at all time indices under consideration (Hannaford & Ryu, 2002).

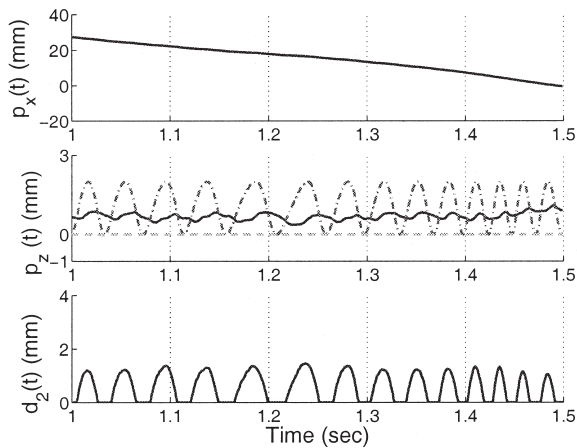
Figure 11 shows representative data plots for the following four cases: (a) the haptic texture-rendering system was passive (hence stable) and participant reported no perceived instability during free exploration; (b) the



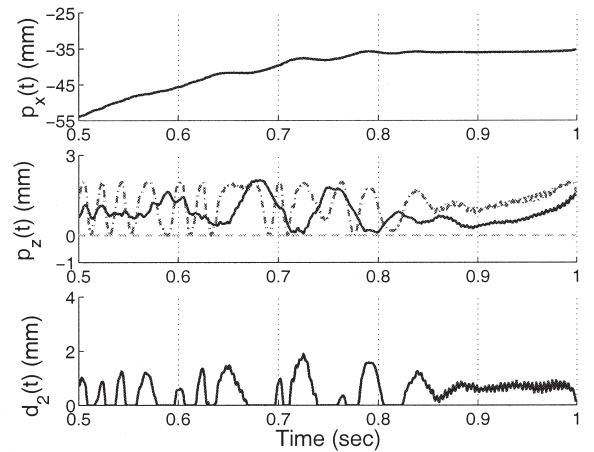
(a) Stable stroking of textures rendered with $d_1(t)$ [$\mathbf{F}_{vec}(t)$ and $K = 0.15$ N/mm].



(b) Unstable stroking of textures rendered with $d_1(t)$ [$\mathbf{F}_{mag}(t)$ and $K = 0.4$ N/mm].



(c) Unstable stroking of textures rendered with $d_2(t)$ [$\mathbf{F}_{mag}(t)$ and $K = 0.6$ N/mm].



(d) Unstable stroking of textures rendered with $d_2(t)$ [$\mathbf{F}_{vec}(t)$ and $K = 1.2$ N/mm].

Figure 9. PHANToM stylus trajectories during stroking of textured surfaces rendered with different collision-detection algorithms and texture-rendering methods. All panels show data collected from S1 when he stroked the same textured surfaces ($A = 1$ mm and $L = 2$ mm).

rendering system was passive and aliveness was perceived during free exploration; (c) the rendering system was passive and aliveness was perceived during stroking; and (d) the rendering system was active and both buzzing and aliveness were perceived during stroking. The top

two panels show $p_z(t)$ (position in the z -direction along surface-height variation), $\mathbf{F}_z^W(t)$ (force in the z -direction), and PO, recorded over 10 s. The bottom two panels show an additional trace of $p_x(t)$ (position along the direction of stroking).

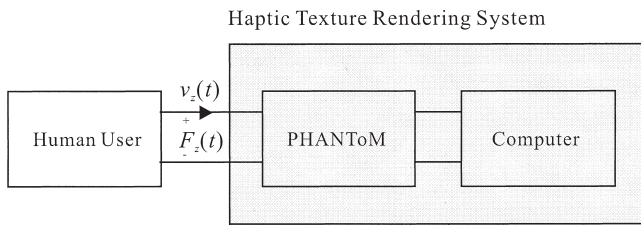


Figure 10. Definition of force and velocity used for the passivity analysis.

It can be seen from Figure 11(a) that the participant was able to maintain a stationary contact between the PHANToM stylus and the virtual textured surface. Both the position and force traces exhibited no obvious abrupt changes at any time. The PO plot remained positive at all times, indicating that the haptic texture-rendering system was passive and stable. These data were taken with a stiffness value that was about one standard deviation below the threshold for perceptually stable texture rendering under the same condition. This was an example of a haptic texture-rendering system that was stable in both perception and control.

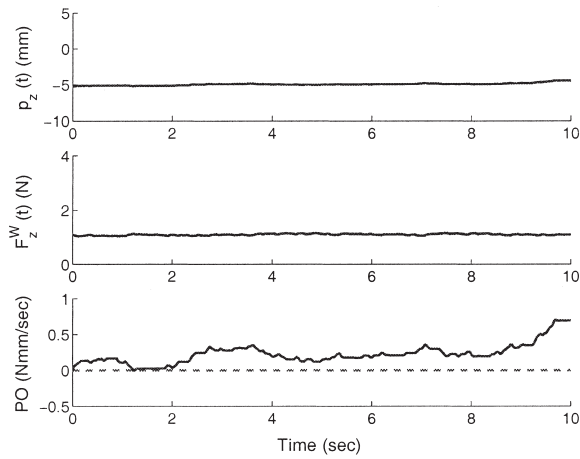
Figure 11(b) shows data measured with a stiffness value that was about one standard deviation above the threshold for stable rendering. The participant reported the perception of aliveness in this case. Consistent with the participant's perception, large fluctuations were observed in both the $p_z(t)$ and $F_z^W(t)$ traces. However, excluding the data in the 3–5-s time interval that seemed to be the result of the participant's voluntary movement, the position change in $p_z(t)$ was relatively smaller (about 2 mm at maximum) than the force change in $F_z^W(t)$ (about 1 N at maximum) over the 10-s time period. Despite the perception of aliveness, however, the PO remained positive, indicating that the texture-rendering system was passive and stable. This was an example of perceived instability despite a stable haptic texture-rendering system.

A similar case was found with stroking mode. The data shown in Figure 11(c) were measured with a stiffness value that was one standard deviation above the corresponding threshold for stable texture rendering. The participant reported the perception of aliveness but

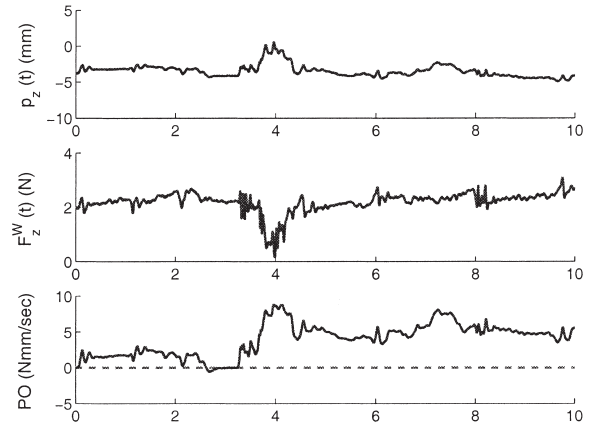
not buzzing. The top trace shows that the participant completed a little more than one complete stroking motion during the 10-s period. The next two traces [$p_z(t)$ and $F_z^W(t)$] show the abrupt changes in proximal stimuli that resulted in the perception of aliveness. In particular, the magnitude of force variations was up to about 2 N. Despite the perception of aliveness, however, the PO remained positive, indicating that the texture-rendering system was passive and stable. This was yet another example of perceived instability despite a stable haptic texture-rendering system.

Figure 11(d) shows an example of an active texture-rendering system during stroking. The data were measured when the participant stroked the textured surface rendered with a high stiffness value ($K = 1.2$ N/mm). The participant reported both types of perceived instability (aliveness and high-frequency buzzing noises). Aliveness can be observed in the two traces of $p_z(t)$ and $F_z^W(t)$ in terms of very small positional variations but relatively large force variations. High-frequency buzzing was confirmed by a spectral peak at 150 Hz in the power spectrum of $p_z(t)$ that was shown earlier in Figure 7(b). In the bottom trace of Figure 11(d), the PO was mostly negative, indicating that the texture-rendering system was active (and hence possibly unstable).

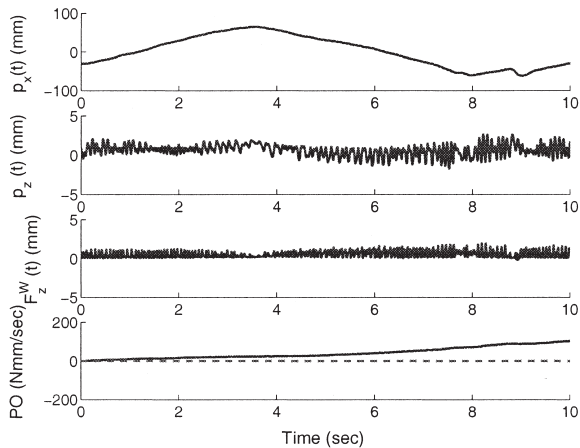
These results provide unequivocal evidence that perceived instability can occur even when a rendering system is passive and stable. We have therefore shown indirectly that environment modeling and human perception can also play important roles in perceived quality of a haptic texture-rendering system. Consider the difference between touching a real and a virtual rigid surface. When a stylus touches a real surface, it is either on or off the surface. When a stylus touches a virtual surface, however, the stylus has to penetrate the virtual surface in order for the user to form a perception of that surface through the resultant force variations. With a real surface, a stylus resting on the surface can remain stationary due to friction (and the fact that the surface cannot be penetrated by the stylus). With a virtual surface, however, the stylus's position can fluctuate inside the surface. This position variation can be amplified into perceivable force variations by the texture renderer, thereby contributing to the perception of aliveness. In



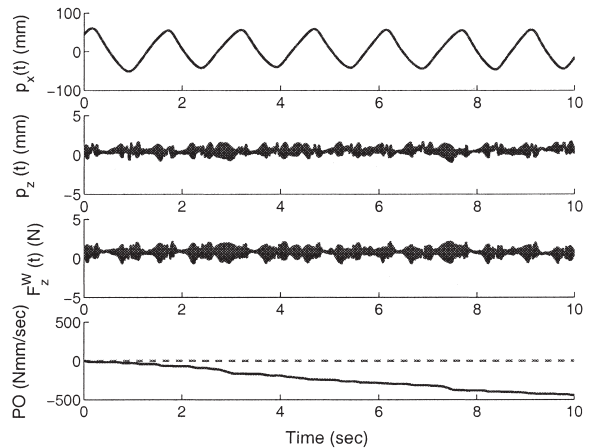
(a) A passive haptic texture rendering system without perceived instability (S2, free exploration, $A = 1$ mm, $L = 2$ mm, and $K = 0.2$ N/mm).



(b) A passive haptic texture rendering system with aliveness perception (S1, free exploration, $A = 1$ mm, $L = 2$ mm, and $K = 0.5$ N/mm).



(c) A passive haptic texture rendering system with aliveness perception (S1, stroking, $A = 1$ mm, $L = 2$ mm, and $K = 0.8$ N/mm).



(d) An active haptic texture rendering with both types of perceived instability (S2, stroking, $A = 1$ mm, $L = 2$ mm, and $K = 1.2$ N/mm).

Figure 11. Passivity analysis of haptic texture-rendering system under four conditions: (a) passive system without perceived instability; (b) passive system with aliveness perception; (c) passive system with aliveness perception; (d) active system with both aliveness and buzzing perception.

addition to the effect of inaccurate environment modeling, human perceptual resolution also plays an important role in the perception of aliveness. It is now well

known in the literature that we tend to rely more on vision for position/movement information, and that we can easily integrate visual position information with hap-

tic force information (e.g., Srinivasan, Beauregard, & Brock, 1996). Our relatively poor kinesthetic resolution of unsupported hand movements in free space combined with our relatively high sensitivity to force changes is also to blame for the perception of aliveness.

5 Conclusions

This study investigated the effect of the collision-detection algorithm on the perceived instability of the virtual haptic texture. It was a follow-up of a previous study where we quantified the parameter space for perceptually stable haptic texture rendering and explored the sources of perceived instabilities (Choi & Tan, 2004). The main difference between our previous and present studies was the way collision detection was performed. The new algorithm [$d_2(t)$] used in this study removed the step changes in force magnitude that could have contributed to perceived instability in our previous study. The results from the present psychophysical experiments showed a significant increase in the stiffness threshold (maximum stiffness under which virtual haptic textures were perceived to be stable) for three of the four experiments conducted (Experiments I, II, and IV). Virtual textures rendered in Experiment III were perceived to be so unstable that the estimated stiffness thresholds were close to 0 for all practical purposes. The results from the present measurement experiments indicated that buzzing (caused by high-frequency noises) was still a dominant form of perceived instability. A new type of perceived instability, aliveness, was also identified. Our analysis suggested that aliveness was caused by a relatively large change in force magnitude calculated from a relatively small change in the stylus position. We hypothesize that since the participant was under the impression that the stylus was held stationary in space, this force variation was attributed to an alive textured surface rather than the slight tremor of the participant's hand. Furthermore, we showed that the perception of aliveness could occur even when the haptic texture-rendering system was passive (and therefore stable in the control sense) using a passivity-based control theory. To the best of our knowledge, this is the first time that any-

one has demonstrated that the perceptual artifacts associated with a haptic rendering system cannot be attributed to control instabilities alone.

When a virtual haptic environment is rendered, at least three factors need to be taken into consideration in order for the virtual objects to feel realistic and stable: environment modeling, control stability, and haptic perception. Several conclusions can be drawn from our present and previous studies in this context. First, much improvement is still needed in the area of haptic texture rendering. Although the new collision-detection algorithm used in the current study has resulted in a significant increase in the maximum stiffness values that can be applied, the numerical range of texture model parameters for perceptually stable haptic texture rendering is still very limited. The textures rendered in the range feel soft. The maximum stiffness thresholds shown in Figure 4 are much less than that measured for a perceptually stable flat wall without any texture (1.0 N/mm; see Choi & Tan, 2004).

Second, our study continues to show that the high-frequency dynamics of a force-feedback device can be a primary source for the perception of buzzing during haptic texture rendering. Typically, control-based studies for stable haptic interaction focus on the low-frequency dynamics of a haptic interface, since the target virtual environment (e.g., virtual flat wall) is expected to involve relatively low-frequency force commands. What we have shown in our studies is that the high-frequency dynamics can no longer be ignored in texture rendering where relatively fast and abrupt changes in force magnitude/direction can occur.

Third, this study provides unequivocal evidence that, unlike the case of virtual wall rendering, both the haptic texture-rendering method (spring method) and the virtual texture model (sinusoidal grating) can potentially lead to the perception of unrealistic sensations such as aliveness while the haptic interface is stably controlled. Therefore, the development of a haptic texture-rendering system needs to incorporate perceived instability as one of its design requirements in addition to the traditionally considered performance metrics such as computational efficiency and control stability.

In the future, we will continue to examine the effect

of other factors (such as damping, friction, and haptic update rate) on the perceived quality of a haptic texture-rendering system. In addition, we will tackle the difficult problem of extending the techniques that have been developed for stable virtual-wall rendering to the area of texture rendering.

Acknowledgments

This work was supported in part by a National Science Foundation (NSF) Faculty Early Career Development (CAREER) Award under Grant 9984991-IIS and in part by an NSF award under Grant 0098443-IIS. The authors wish to thank Blake Hannaford and Jee-Hwan Ryu for discussion on passivity observer, Vincent Hayward for discussion on velocity estimation, Zygmunt Pizlo for discussion on data analysis, and the three anonymous reviewers for their thoughtful comments.

References

- Adams, R. J., & Hannaford, B. (1999). Stable haptic interaction with virtual environments. *IEEE Transactions on Robotics and Automation*, 15(3), 465–474.
- Cavuşoğlu, M. C., Feygin, D., & Tendick, F. (2002). A critical study of the mechanical and electrical properties of the PHANTOM haptic interface and improvements for high performance control. *Presence: Teleoperators and Virtual Environments*, 11(6), 555–568.
- Cavuşoğlu, M. C., Sherman, A., & Tendick, F. (2002). Design of bilateral teleoperation controllers for haptic exploration and telemanipulation of soft environments. *IEEE Transactions on Robotics and Automation*, 18(4), 641–647.
- Choi, S., & Tan, H. Z. (2004). Perceived instability of virtual haptic texture. I. Experimental studies. *Presence: Teleoperators and Virtual Environments*, 13(4), 395–415.
- Costa, M. A., & Cutkosky, M. R. (2000). Roughness perception of haptically displayed fractal surfaces. *Proceedings of the ASME Dynamic Systems and Control Division*, 69(2), 1073–1079.
- Fritz, J. P., & Barner, K. E. (1996). Stochastic models for haptic texture. *Proceedings of SPIE's International Symposium on Intelligent Systems and Advanced Manufacturing—Telemanipulator and Telepresence Technologies III*, 34–44.
- Gillespie, R. B., & Cutkosky, M. R. (1996). Stable user-specific haptic rendering of the virtual wall. *Proceedings of the ASME International Mechanical Engineering Congress and Exhibition*, 58, 397–406.
- Hannaford, B., & Ryu, J.-H. (2002). Time-domain passivity control of haptic interfaces. *IEEE Transactions on Robotics and Automation*, 18(1), 1–10.
- Ho, C., Basdogan, C., & Srinivasan, M. A. (1999). Efficient point-based rendering techniques for haptic display of virtual objects. *Presence: Teleoperators and Virtual Environments*, 8(5), 477–491.
- Ho, P. P., Adelstein, B. D., & Kazerooni, H. (2004). Judging 2D versus 3D square-wave virtual gratings. *Proceedings of the 12th International Symposium on Haptic Interfaces for Virtual Environment and Teleoperator Systems*, 176–183.
- Janabi-Sharifi, F., Hayward, V., & Chen, C.-S. J. (2000). Discrete-time adaptive windowing for velocity estimation. *IEEE Transactions on Control System Technology*, 8(6), 1003–1009.
- Kim, L., Kyrikou, A., Sukhatme, G. S., & Desbrun, M. (2002). An implicit-based haptic rendering technique. *Proceedings of the IEEE/RSJ International Conference on Intelligent Robots and Systems*, 2943–2948.
- Lawrence, D. A., Pao, L. Y., Dougherty, A. M., Salada, M. A., & Pavlou, Y. (2000). Rate-hardness: A new performance metric for haptic interfaces. *IEEE Transactions on Robotics and Automation*, 16(4), 357–371.
- Lederman, S. J., Klatzky, R. L., Hamilton, C. L., & Ramsay, G. I. (1999). Perceiving roughness via a rigid probe: Psychophysical effects of exploration speed and mode of touch. *Haptics-e*, 1(1). Available from: <http://www.haptics-e.org>.
- Lin, M. C., & Manocha, D. (2004). Collision and proximity queries. In E. Goodman & J. O'Rourke (Eds.), *Handbook of discrete and computational geometry* (pp. 787–808). Boca Raton, FL: CRC Press.
- Massie, T. H. (1996). *Initial haptic explorations with the PHANTOM: Virtual touch through point interaction*. Unpublished master's thesis, Massachusetts Institute of Technology, Cambridge, MA.
- Miller, B. E., Colgate, E., & Freeman, R. A. (2000). Guaranteed stability of haptic systems with nonlinear virtual environments. *IEEE Transactions on Robotics and Automation*, 16(6), 712–719.
- Minsky, M., & Lederman, S. J. (1996). Simulated haptic textures: Roughness. *Proceedings of the ASME Dynamic Systems and Control Division*, 58, 421–426.

- Okamura, A. M., Dennerlein, J. T., & Howe, R. D. (1998). Vibration feedback models for virtual environments. *Proceedings of the IEEE International Conference on Robotics and Automation*, 674–679.
- Siira, J., & Pai, D. K. (1996). Haptic texturing—a stochastic approach. *Proceedings of the IEEE International Conference on Robotics and Automation*, 557–562.
- Srinivasan, M. A., Beaugard, G. L., & Brock, D. L. (1996). The impact of visual information on haptic perception of stiffness in virtual environments. *Proceedings of the ASME Dynamic Systems and Control Division*, 58, 555–559.
- Verrillo, R. T. (1963). Effect of contactor area on the vibrotactile threshold. *Journal of the Acoustical Society of America*, 35(13), 1962–1966.
- Wall, S. A., & Harwin, W. S. (1999). Modeling of surface identifying characteristics using Fourier series. *Proceedings of the ASME Dynamic Systems and Control Division*, 67, 65–71.
- Weisenberger, J. M., Krier, M. J., & Rinker, M. A. (2000). Judging the orientation of sinusoidal and square-wave virtual gratings presented via 2-DOF and 3-DOF haptic interfaces. *Haptics-e*, 1(4). Available from: <http://www.haptics-e.org>.